



Methodology for measuring the thermal conductivity of insulating samples with small dimensions by heat flow meter technique

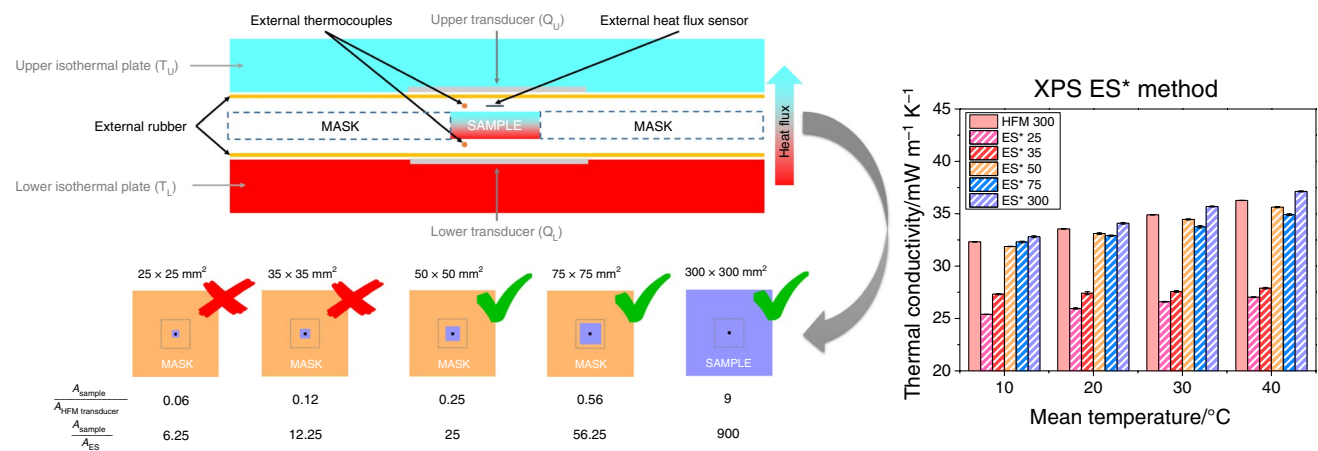
Ismael Sánchez-Calderón¹ · Beatriz Merillas¹ · Victoria Bernardo² · Miguel Ángel Rodríguez-Pérez^{1,3}

Received: 22 September 2021 / Accepted: 16 June 2022
© The Author(s) 2022

Abstract

Nowadays, developing advanced, highly insulating materials for minimizing heat losses in buildings is of utmost relevance. Thus, there is a constant research activity focused on developing new and enhanced solutions for thermal insulation. However, characterizing the behavior of new thermal insulation materials, usually produced at lab-scale with small dimensions, by a steady-state approach is a challenge. The reason is that commercial heat flow meters require large samples (hundred on mm side) to provide accurate results of thermal conductivity because they are based on international standards. In this work, a new methodology to measure the thermal conductivity of small prototypes of thermal insulating materials (as low as $50 \times 50 \text{ mm}^2$) is developed by using an external heat flux sensor placed into a standard heat flow meter apparatus. Four different thermal insulators were used to validate the developed methodology by performing measurements in the heat flow meter with and without the external sensor. From these results, a calibration curve that relates both methods was calculated. Furthermore, the effect of the sample size was studied to explore the limits of the technique. Results show that the self-developed method is an accurate procedure to determine the thermal conductivity of samples with small dimensions via a steady-state condition.

Graphical abstract



Keywords Thermal conductivity · Heat flux · Heat flux sensor · Heat flow meter · Thermal insulator

Introduction

Nowadays, the efficient use of energy is one of the main concerns of our society. All sectors require efficient management of energy use, but, according to the European Commission [1], the main challenge for the coming decades

✉ Ismael Sánchez-Calderón
ismaelsc@fmc.uva.es

Extended author information available on the last page of the article

will be in buildings. More than a third of the global energy consumption is used in buildings, and of this energy, more than 50% is needed to heat interior spaces. Most of the heat is lost through walls, ceilings, and floors. Therefore, adequate insulation is required to reduce heat losses and, thus, energy consumption. Improved thermal insulators would save money and also would significantly reduce the CO₂ emissions associated with energy production. In this way, finding new materials with enhanced insulation properties becomes a mandatory task, and significant research in this field is ongoing. However, most of the research carried out at laboratory scale results in the production of small samples of thermal insulating samples that are difficult to characterize [2–5], as is explained in the following paragraphs.

Insulation materials are characterized by their thermal conductivity (λ). Thermal conductivity is an intensive physical property of materials that describes heat transport through a body due to a temperature gradient. Thermal conductivity can span several orders of magnitude, from vacuum insulation panels (0.004 W m⁻¹ K⁻¹) to single-layer graphene (3000 W m⁻¹ K⁻¹) [6, 7]. For materials currently used in the thermal insulation sector, typical values are in the range of 20–40 mW m⁻¹ K⁻¹ for insulators like rigid polyurethane foam (PUR), mineral wool, expanded polystyrene foam (EPS), and extruded polystyrene foam (XPS).

The thermal conductivity of a material is its ability to transfer heat. It is defined via Fourier's law of thermal conduction (Eq. (1)). This equation states that the time rate of heat flux density through a material (\vec{q}) is proportional to the negative gradient in the temperature ($\vec{\nabla}T$), and λ is the parameter relating to both factors. The heat flux density is defined as the time rate of heat transfer per unit area normal to the direction of heat transfer. It is a vector quantity since it has both direction and magnitude. According to the second law of thermodynamics, heat always flows in the direction of the lower temperature. Regarding thermal conductivity, it is usually considered as a scalar (a constant). Still, in some cases, it can vary with local position or direction (such as in anisotropic or heterogeneous materials). For the data analysis of this work, λ will be considered as a constant parameter only depending on the material type and temperature of measurement.

$$\vec{q} = -\lambda \vec{\nabla}T \quad (1)$$

When measuring the thermal conductivity, it is possible to distinguish between transient and steady-state techniques depending on how Eq. (1) is solved. On the one hand, in transient or non-steady-state methods, the temperature distribution throughout the sample varies with time. In this case, solving the heat conduction equations is more complicated because it involves a time-dependent heat flow equation [8]. One interesting advantage of these techniques is that

measurements can be performed in small samples; however, the accuracy of these methods for thermal insulating materials is not clear [9, 10]. For instance, in the work of Zheng et al. [10] it is proved that complex calculations are required to fit the TPS data to more realistic values as those obtained in steady-state techniques. On the other hand, in steady-state methods, a temperature difference that does not evolve with time is established; thus, the mathematics are simplified, turning the heat transfer problem into a one-dimensional problem. A steady-state condition is attained when the heat flux through the sample is constant, i.e., the temperature at each point of the specimen does not vary over time (see Fig. 1) [6].

Equation (2) is the one-dimensional solution of Fourier's law for a steady-state method. It allows the calculation of the thermal conductivity in W m⁻¹ K⁻¹, where q is the heat flow throughout the sample per unit area in W m⁻², Q ($Q = q \cdot A$) is the heat flow throughout the sample in W, A is the area the heat flow passes through in m², d is the sample's thickness in m, T_2 is the temperature of the cold source, T_1 is the temperature of the hot source, and ΔT ($\Delta T = T_1 - T_2$) is the temperature difference across the sample in K.

$$q = -\lambda \frac{dT}{dx} \rightarrow q \int_{T_1}^{T_2} dT = -\lambda \int_0^d dx \rightarrow q(T_2 - T_1) = -\lambda d \rightarrow \quad (2)$$

$$\lambda = \frac{q \cdot d}{T_1 - T_2} = \frac{Q \cdot d}{A \cdot \Delta T}$$

Both methods, either transient or steady, have advantages and limitations, and they are suitable for only a limited range of materials, depending on the thermal properties, sample configuration, and measuring temperature [6, 7]. For instance, transient measurements are relatively quicker than steady-state measurements, where the time until the thermal equilibrium is reached can be rather long. However, non-steady approaches are typically indirect, which adds additional uncertainties to the measurement. For this reason, they are not the ideal techniques for characterizing insulating

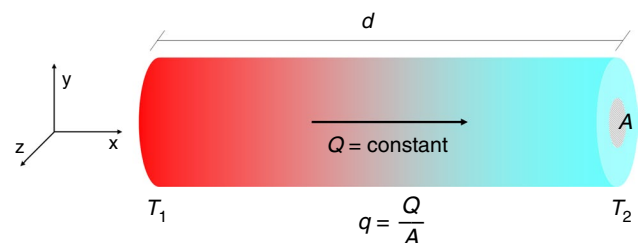


Fig. 1 Steady-state condition scheme of heat transfer between two sources at temperatures T_1 and T_2 that are maintained constant during the experiment across a sample of thickness d

materials, described by very low thermal conductivities in which any uncertainty can have a great effect [11].

To measure the thermal conductivity of insulators, steady-state techniques, like guarded hot plate and heat flow meters, are commonly used [6]. There are several international standards, very common in the industry to carry out these measurements, such as ASTM C518 [12] and ISO 8301 [13] for heat flow meters, and ASTM C177 [14], ISO 8302 [15], or UNE-EN 12667 [16] for guarded hot plate meters. On the two steady techniques, the heat flows from a hot plate (at temperature T_1), throughout the sample, to a cold plate (at temperature $T_2 < T_1$), establishing a temperature gradient (as shown in Fig. 1). After reaching the thermal equilibrium, the heat flow Q and the temperature difference across the sample ($\Delta T = T_1 - T_2$) are measured. Thermal conductivity is calculated by using Fourier's law one-dimension solution (Eq. (2)), introducing the sample thickness (d).

The guarded hot plate method is considered an absolute method because the heat flux is determined by measuring the power to keep the temperature of the hot plate constant [6, 7]. On the contrary, the heat flow meters are a comparative or relative method [6, 7]. In this case, the heat flux is determined by measuring the voltage drop through an electrical resistor, a so-called sensor or heat flux transducer, which is previously calibrated. While the guarded hot plate is a very time-consuming apparatus, heat flow meters are faster and provide accurate measurements. Thus, the latter is the most commonly used apparatus to determine the conductivity of insulation materials.

At lab-scale, the main problem of these steady-state techniques resides in the large samples that are needed to perform the measurements. The steady-state equipments are designed to fulfill the requirements of the international standards (such as ASTM C518 [12] or ISO 8301 [13]), for which large samples are mandatory. Typical heat flow meters measure samples of $300 \times 300 \text{ mm}^2$, while the measuring area where the heat flow sensor is located is higher than $100 \times 100 \text{ mm}^2$. Thus, researchers have been developing new methods to measure small-size samples [11, 17–19]. For instance, Miller et al. [19] developed a hot-plate device to measure the thermal conductivity of small aerogel samples (20 mm diameter and 2.5 mm thickness) with conductivities on the order of that of air (around $26 \text{ mW m}^{-1} \text{ K}^{-1}$). Meanwhile, Jannot et al. [11, 17, 18] continuously improve a centered hot plate method to finally measure centimeter size samples (15 mm diameter and 3–9 mm thickness) accurately. However, these devices are homemade methods with complex technical parts, complicating their scalability to other laboratories. Other researchers tuned their commercial heat flow meters [5], reducing the heat flux transducer area. This approach had the advantage of using most of the parts of a commercial heat flow meter, but it has the main drawback of disassembling the equipment to add the smaller sensor.

Following the previous ideas, in this work, a new methodology to measure the thermal conductivity of small samples has been developed by using an external heat flow sensor ($10 \times 10 \text{ mm}^2$ of area) in combination with a commercial heat flow meter. The sensor is installed on top of the sample externally, so no modifications to the equipment are needed, and the method can be easily implemented in any heat flow meter. By this approach, and thanks to the small area of the sensor, small samples can be measured with good accuracy within the temperature range of the sensor.

Experimental

Materials and sample preparation

Four well-known thermal insulating foam materials were used in this work to test the method. The characteristics of the samples are listed in Table 1. The materials are an extruded polystyrene foam (XPS), an expanded polystyrene foam board (EPS), a rigid polyurethane foam (PUR), and a polyethylene foam (PE). The density of the samples was determined by the geometric method. The cell size was characterized with a self-developed tool in the software ImageJ [20]. The range of density of these products varies from 17 to 41 kg m^{-3} , while the cell sizes are in the range from 120 to $700 \text{ }\mu\text{m}$.

Initially, samples were cut in $300 \times 300 \text{ mm}^2$ sheets with a thickness of 15 mm to measure their thermal conductivity using the standard heat flow meter procedure and the external sensor approach.

From the samples used in the previous analysis, smaller samples were cut to investigate the effect of the sample size. First, samples of XPS with dimensions of 25×25 , 35×35 , 50×50 , and $75 \times 75 \text{ mm}^2$ were used to analyze the resolution of the method regarding the sample size. The rest of the materials (PE, EPS, and PUR) were cut in dimensions of $50 \times 50 \text{ mm}^2$ to compare the obtained results and to confirm the validity of the method for small samples. A PUR mask (density of 36 kg m^{-3} and thermal conductivity of $26.26 \text{ mW m}^{-1} \text{ K}^{-1}$ at $20 \text{ }^\circ\text{C}$) was used for these measurements to fill the remaining volume of the heat flow meter, avoiding convection.

Table 1 Density and cell size of the thermal insulators used in this work

Material	Density/ kg m^{-3}	Cell Size/ μm
XPS	34	140
EPS	17	120
PUR	33	200
PE	41	700

Thermal conductivity measurements

Commercial heat flow meter (HFM)

Thermal conductivity measurements were performed using a thermal heat flow meter model FOX 314 (TA Instruments/LaserComp, Inc.), which measures according to ASTM C518 and ISO 8301 [12, 13]. Samples with dimensions $300 \times 300 \times 15 \text{ cm}^3$ (width \times length \times thickness) were used. For the measurements, the sample was placed between the two plates, promoting a temperature gradient through the material thickness (Fig. 2a). The measurements were performed at 10, 20, 30, and 40 °C. The temperature gradient (ΔT) was set to 20 °C in every case (i.e., for the measurement at 10 °C, the temperature goes from 0 °C in the upper isothermal plate to 20 °C in

the lower one). The active area of the FOX 314 heat flux transducers is $100 \times 100 \text{ mm}^2$, and the absolute thermal conductivity accuracy is 2%.

In the measurements of this work, the commercial heat flow meter performs cycles of 512 s and calculates the average thermal conductivity of each cycle. The steady-state condition (i.e., the conductivity does not vary with time) is reached after 2–3 cycles. Once the steady-state condition is reached, the commercial heat flow meter performs 8 additional cycles (set by user). Finally, the mean thermal conductivity and the standard deviation are calculated from the last 3 cycles (set by user). Up to precision, note that once the steady-state condition is reached, the thermal conductivity value provided each cycle is almost the same.

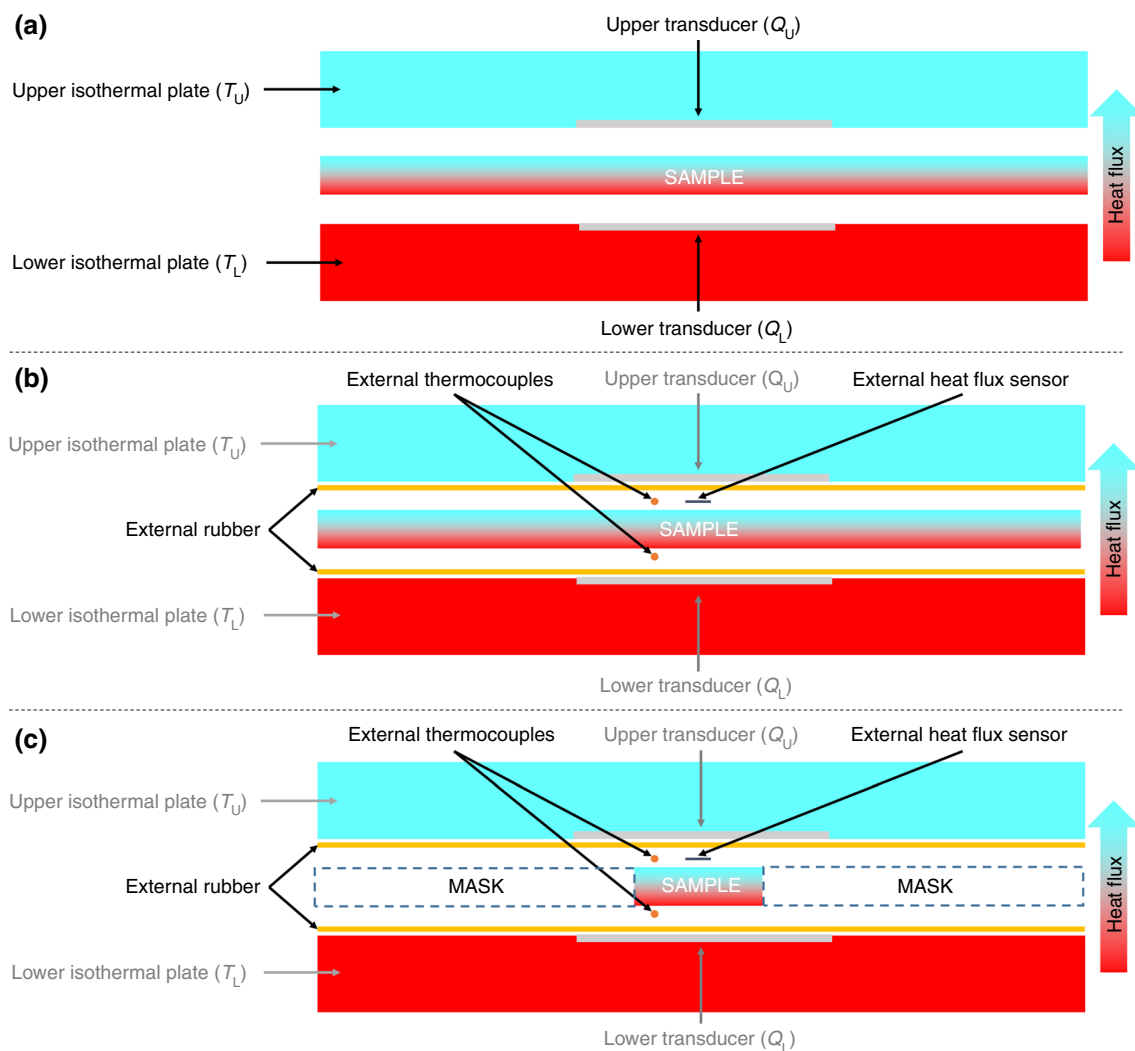


Fig. 2 Scheme of the measurement procedure to determine the thermal conductivity using: **a** a commercial heat flow meter for samples of $300 \times 300 \text{ mm}^2$; **b** an external sensor coupled to a commercial

heat flow meter for samples of $300 \times 300 \text{ mm}^2$; and **c** an external sensor coupled to a commercial heat flow meter for samples of dimensions $< 100 \times 100 \text{ mm}^2$.

External sensor coupled to a commercial heat flow meter (ES)

Additionally, a heat flux sensor gSKIN®-XP 27 9C (greenTEG AG) and a data logger gSKIN® DLOG-4218 (greenTEG AG) were used to measure the thermal conductivity. This combination allows measuring in a range of $\pm 1100 \text{ W m}^{-2}$. The relative error of the flux measured is 3%. Sensor dimensions are $10 \times 10 \text{ mm}^2$ with a thickness of 0.5 mm. The temperature range of the sensor is from $-50 \text{ }^\circ\text{C}$ to $150 \text{ }^\circ\text{C}$. The sensor is calibrated under steady-state conditions with a method that is oriented towards ISO8301 [21]. A linear correction factor S_c accounts for the temperature dependency of the sensor sensitivity. To calculate the sensitivity of the sensor at temperature T_s Eq. (3) is used, where $S_0 = 10.74 \text{ } \mu\text{V m}^2 \text{ W}^{-1}$ and $S_c = 0.0134 \text{ } \mu\text{V m}^2 \text{ W}^{-1} \text{ }^\circ\text{C}^{-1}$. Equation (3) and the correction factors are provided by greenTEG AG.

$$S(T) = S_0 + (T_s - 22.5) \cdot S_c \quad (3)$$

The heat flux per unit area is finally calculated using the following formula (Eq. (4)), where U is the sensor output voltage in μV .

$$q = \frac{Q}{A} = \frac{U}{S} \quad (4)$$

The measurements using the external sensor were performed using the following method. First, samples of $300 \times 300 \times 15 \text{ mm}^3$ were placed between the two plates of a commercial heat flow meter. As shown in Fig. 2a, in this case, two rubber pieces of dimensions $300 \times 300 \text{ mm}^2$

(thickness 1.5 mm) were placed between the sample and the plates to minimize the fluctuations of the heat flux registered by the sensor. The sensor is located between the sample and the upper rubber piece, in the middle of the samples' surface. Furthermore, two thermocouples were used to monitor the temperature on both sides of the sample. To measure the thermal conductivity of the small samples (samples area < heat flow meter heat flux transducers area), a PUR mask was used to fill the remaining space to avoid convection (Fig. 2b).

For all the experiments using the external sensor, the output voltage was measured every second (Fig. 3a). The output signal has been smoothed to compare the measurements with the ones provided by the commercial heat flow meter, which calculates the average flux at each measuring cycle. An adjacent-averaging smooth has been applied. This smoothing consists of taking the average of a number of data points around each point in the data and replacing that point with the new average value. The number of data points to perform the smooth was set to 400 to compare with the commercial heat flow meter measurements (which calculates the thermal conductivity of each cycle as an average of the values measured during 512 s). Finally, an average of 1200 s (i.e., 3 cycles of the commercial heat flow meter) was taken in the smoothed signal in the region where the steady-state condition is reached (i.e., the voltage does not vary with the time) to obtain the mean output voltage and the standard deviation (Fig. 3b). This data treatment just reduces the measurement fluctuations (i.e., the standard deviation), not affecting the mean value of the calculated thermal conductivity and providing an accurate comparison with the results obtained by the commercial heat flow meter.

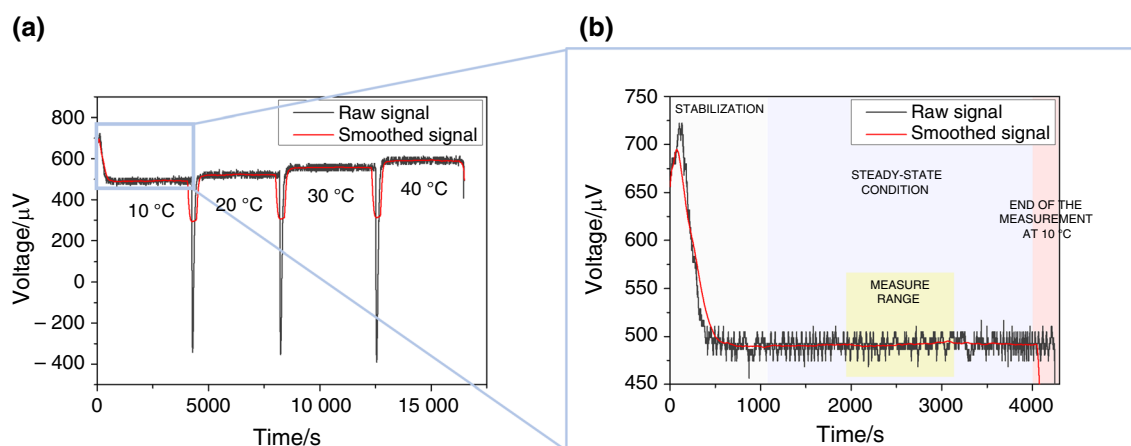


Fig. 3 **a** Example of the sensor output voltage obtained when measuring one sample at four different temperatures. **b** Detail of the results at $10 \text{ }^\circ\text{C}$ and range of data used for calculating the thermal conductivity

Results and discussion

HFM versus ES method

Figure 4 summarizes the thermal conductivities of the XPS, EPS, PE, and PUR samples with dimensions $300 \times 300 \times 15 \text{ mm}^3$ obtained by both methods. Thermal conductivities of those materials ranged between $26.45 \text{ mW m}^{-1} \text{ K}^{-1}$ (PUR measured at $10 \text{ }^\circ\text{C}$) and $39.46 \text{ mW m}^{-1} \text{ K}^{-1}$ (PE measured at $40 \text{ }^\circ\text{C}$), values that are in the range of interest for thermal insulation materials. Generally, the thermal conductivities obtained through both methods are similar and follow the same trends. However, the thermal conductivity obtained using the sensor method (ES) is slightly higher than the one provided by the commercial heat flow meter (HFM). For example, at $20 \text{ }^\circ\text{C}$ for the XPS (Fig. 4a), the HFM method provides $33.55 \text{ mW m}^{-1} \text{ K}^{-1}$, while the ES method gives $35.50 \text{ mW m}^{-1} \text{ K}^{-1}$

$\text{m}^{-1} \text{ K}^{-1}$ (6% increase). For the PUR (Fig. 4c), the difference between the two values is around 7%. Meanwhile, for the EPS and PE samples difference between the two values is around 2%. Differences are slightly higher for XPS and PUR in comparison with EPS and PE samples probably to their higher rigidity which could affect the sample-sensor contact. Also, the relative difference between methods increases as the temperature increases. For instance, for EPS (Fig. 4b) at $10 \text{ }^\circ\text{C}$ the difference between the thermal conductivity obtained through both methods is half of that obtained at $40 \text{ }^\circ\text{C}$ (0.52 versus $1.01 \text{ mW m}^{-1} \text{ K}^{-1}$). Regarding the standard deviation of the measurement (SD) using the ES method is lower than $0.15 \text{ mW m}^{-1} \text{ K}^{-1}$ for most of the materials; meanwhile, using the HFM method is $0.01 \text{ mW m}^{-1} \text{ K}^{-1}$. The SD values are calculated as the deviation of subsequent measurements of the same sample throughout the steady-state regime. However, for the PE (Fig. 4d), the SD is higher in the ES measurements ($0.92 \text{ mW m}^{-1} \text{ K}^{-1}$ at $10 \text{ }^\circ\text{C}$ and $0.31 \text{ mW m}^{-1} \text{ K}^{-1}$ at $40 \text{ }^\circ\text{C}$).

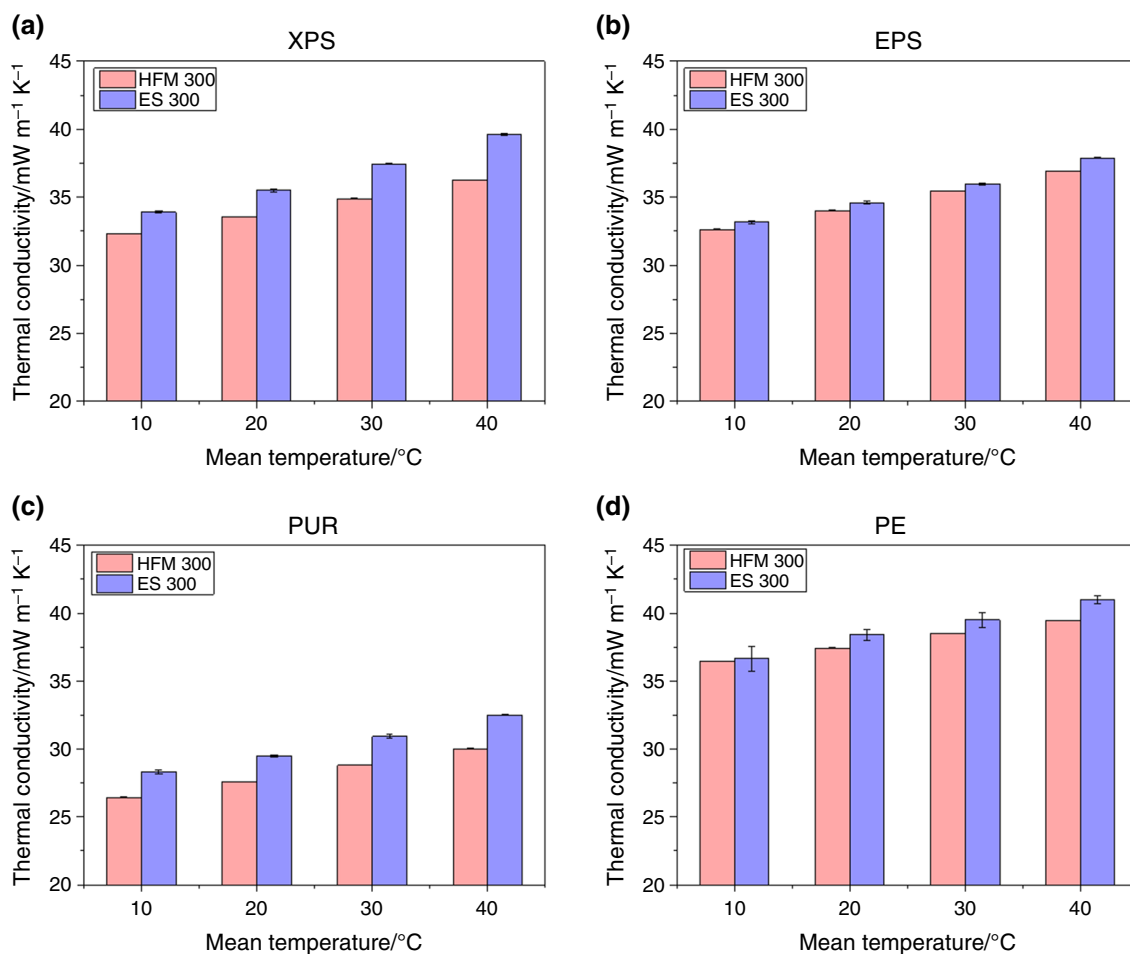


Fig. 4 Comparison between the thermal conductivities obtained by HFM and ES methods for the different samples with 300 mm side (dimensions of $300 \times 300 \text{ mm}^2$): **a** XPS, **b** EPS, **c** PUR, and **d** PE.

Note that the deviation associated with the measurements with the HFM is too low for the resolution of the graphs

Nevertheless, on average, the values measured by the ES method follow the same trends as those obtained with the conventional HFM. On average, differences in the values of the conductivity of 4% are obtained at low temperatures (below 30 °C), while at 40 °C the differences increase up to 6%.

The mean ratio between the thermal conductivity obtained via the two methods ($\lambda_{\text{HFM}}/\lambda_{\text{ES}}$) is represented as a function of the temperature in Fig. 5 to get an average behavior of the relative difference between the methods. The mean ratio has been calculated by averaging the ratio of thermal conductivity ($\lambda_{\text{HFM}}/\lambda_{\text{ES}}$) obtained for each material at each temperature. It is observed that, as previously commented, the ratio decreases as temperature increases; that is, the result obtained with the ES procedure is less similar to the reference HFM value at higher temperatures. A calibration factor (f) as a function of the temperature can be calculated by fitting the data to a linear relation (Fig. 5). This calibration factor correlates the measurements obtained with the ES method to those obtained via the regular HFM method. With

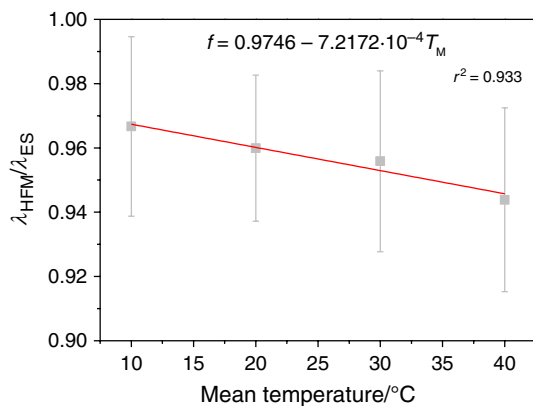


Fig. 5 Mean ratio between the thermal conductivity obtained by the HFM and ES methods as a function of the temperature. Redline: fit of the data (calibration factor f and coefficient of determination of the fit r^2)

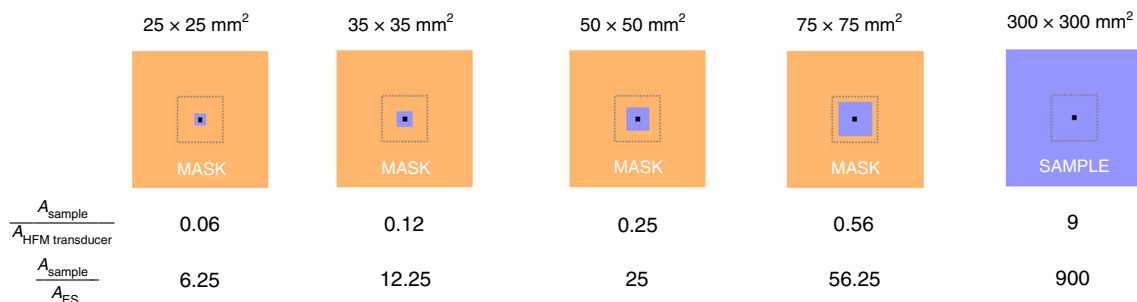


Fig. 6 Sample (purple) - Mask (yellow) configurations scheme to study the effect of the sample size. Dotted line: heat flow meter's heat flux transducers dimensions. Black square: external sensor dimen-

this calibration, it is possible to calculate a corrected thermal conductivity (λ_{ES^*}) using the value obtained with the ES method at any temperature (T_M) from 10 to 40 °C (Eq. (5)). The coefficient of determination (r^2) of the linear fit is 0.933, which implies a good adjustment of the data. This calibration considers the global effect of the employed methodology itself (the use of two external rubber pieces, the external thermocouples, and the external sensor) and allows obtaining a value closer to the one that would have been obtained through the conventional procedure. From now on, results from the ES method after applying the calibration factor would be referred to as ES* method. In the Supporting Information Sect. 1 the results of applying the ES* method to the 300 × 300 mm² samples are presented. Figure S1 shows that the values obtained with the ES* method are almost the same as those measured with the HFM system once the calibration equation of (5) is applied.

$$\lambda_{\text{ES}^*} = f \cdot \lambda_{\text{ES}} = (0.9746 - 7.2172 \cdot 10^{-4} T_M) \cdot \lambda_{\text{ES}} \quad (5)$$

Effect of the sample size using the ES method

XPS was selected to carry out the study of the influence of the sample size on the ES method. Samples of 25 × 25, 35 × 35, 50 × 50, and 75 × 75 mm² were used for this study. A rigid PUR mask was used to fill the remaining volume avoiding convection, as explained in Fig. 2c. Figure 6 presents a scheme of the relative areas of the sample and the PUR mask for the different experiments. Also, the dimensions of the heat flux transducers of the heat flow meter equipment used (dotted line) and sensor (black square) are included to consider the reduction of the sample size and the relationship between the full sample (300 × 300 mm²) and the commercial heat flux transducers of the heat flow meter is 9. The sample-mask configurations for the measurements using the external sensor have been selected to satisfy, in

Under the scheme: area relation between sample and heat flux sensor in each case

most of the cases, this relation (area ratio higher than 9) with the external sensor. The sample with dimensions of $25 \times 25 \text{ mm}^2$ is the exception having a relation of 6.25 between the sample and the external sensor area.

Figure 7 shows the thermal conductivities of the XPS samples as a function of their dimensions at the four temperatures used in this study. The values obtained by the ES method (Fig. 7a) and the ES* method (Fig. 7b) are presented. The value obtained with the HFM technique in a $300 \times 300 \text{ mm}^2$ sample is also included as a reference. Also, the relative difference between the reference thermal conductivity measured by HFM and obtained using the ES method (Fig. 7c) or the ES* method (Fig. 7d) is included. By applying the correction, the accuracy of the measurement improves for all the temperatures (i.e., the relative difference is reduced).

As the sample size decreases, the thermal conductivity maintains almost constant and close to the reference value until reaching a limit. For sample dimensions smaller than $50 \times 50 \text{ mm}^2$, the thermal conductivity drastically decreases to values much lower than the reference value obtained with

the HFM method due to a heat flux reduction. For instance, at 10°C the thermal conductivity for the $50 \times 50 \text{ mm}^2$ sample measured by the ES* method is only 1% higher than the reference. However, the thermal conductivity value is reduced by c.a. $5 \text{ mW m}^{-1} \text{ K}^{-1}$ when passing to $35 \times 35 \text{ mm}^2$ (difference of 15%). We hypothesize that the reduction in the measured heat flux using the external sensor might be because of heat flux losses in the sample produced by border effects.

To summarize, with the current configuration, samples with sizes as small as $50 \times 50 \text{ mm}^2$ can be measured with the external sensor method with high accuracy (relative difference below 4%). Thus, the sensor method allows measuring the thermal conductivity of small-size samples.

Validation of the method

Finally, to validate the method, the thermal conductivity of the rest of the samples (EPS, PUR and PE) with dimensions of $50 \times 50 \text{ mm}^2$ was measured. Figure 8a, b,

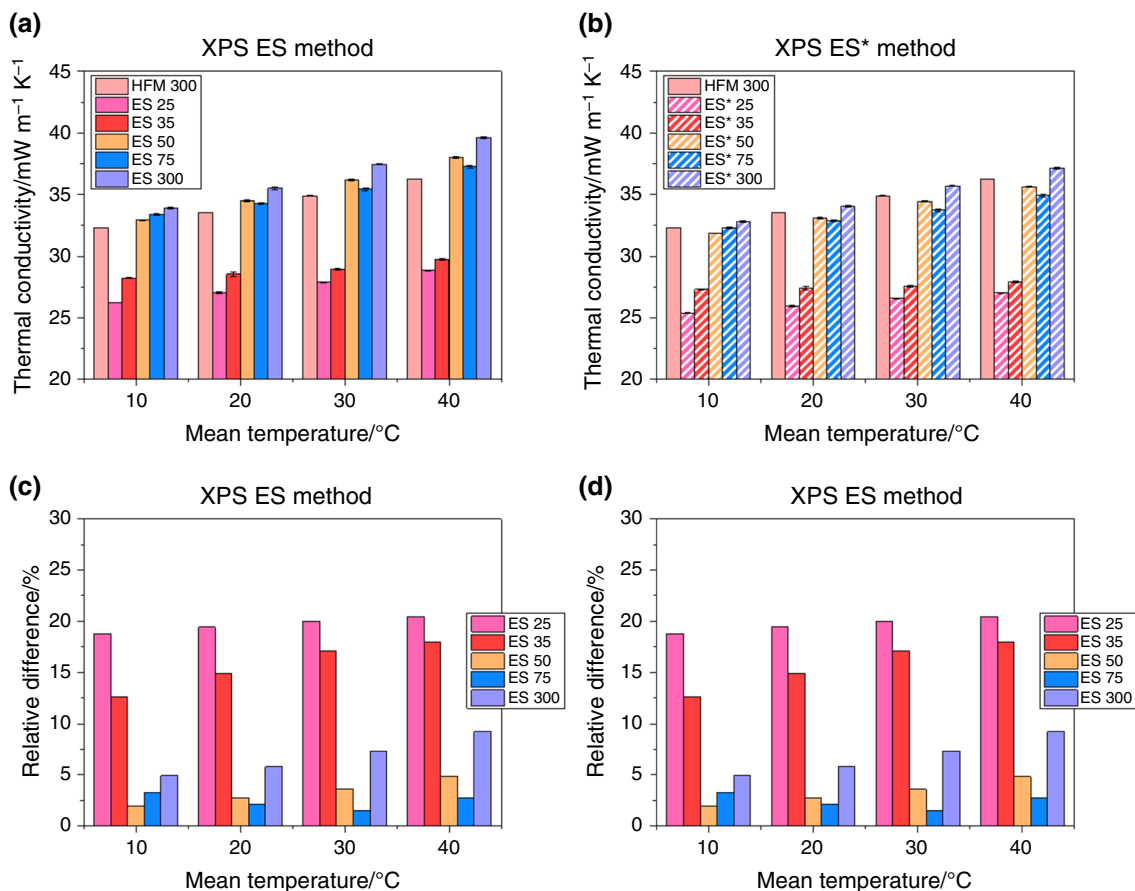


Fig. 7 Influence of the sample size on the thermal conductivity for XPS samples measured at four temperatures using: **a** the ES method and **b** the ES* method. The value obtained via the HFM technique is also included as a reference. The relative difference of the meas-

urements for the **c** ES method and **d** ES* method compared with the HFM value. The number accompanying the method means the sample side in mm

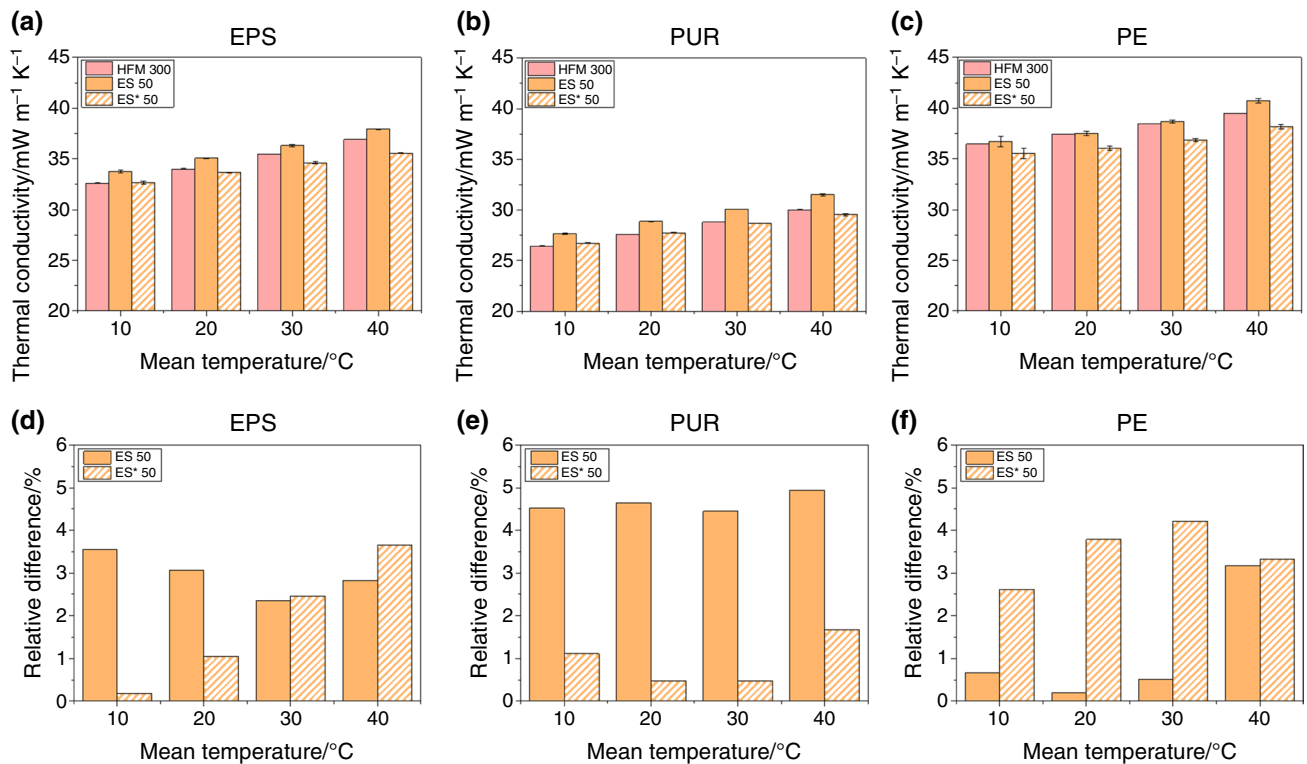


Fig. 8 Comparison between the thermal conductivities obtained by ES and ES* methods for the different samples with 50 mm side (dimensions of $50 \times 50 \text{ mm}^2$): **a** EPS, **b** PUR, and **c** PE. The value obtained via the HFM technique is also included as a reference. The

ES and ES* methods relative difference with respect to the reference value (HFM) for the different samples is presented in **d** EPS, **e** PUR, and **f** PE

and **c** show the calculated thermal conductivities with and without the application of the correction (ES and ES* methods, respectively); for the sake of comparison, the reference value measured with the conventional HFM method is also included. Figure 8d, e, and f present the relative difference between the ES methods and the value obtained with the HFM procedure. For example, at 10°C the EPS $50 \times 50 \text{ mm}^2$ sample shows a value of $33.79 \text{ mW m}^{-1} \text{K}^{-1}$ when the reference value is $32.63 \text{ mW m}^{-1} \text{K}^{-1}$ (Fig. 8a). When applying the correction, the relative difference is reduced and almost 0% (Fig. 8d). Meanwhile, for the PUR (Fig. 8e), the relative difference between measurements decreases from 4 to 1% using the ES* method. However, for the PE foam (Fig. 8c and f), the differences are higher. Anyway, the obtained thermal conductivity is close to the reference value; and the gap between the results is acceptable, taking into account the error of the technique (the absolute error of the HFM is 2% and the relative error of the external heat flux sensor is 3%). Therefore, in general, by applying the correction, the accuracy of the thermal conductivity results improves.

Conclusions

A method to measure the thermal conductivity of small samples using a heat flux sensor with a dimension of $10 \times 10 \text{ mm}^2$ has been developed. The external heat flux sensor is coupled to a commercial heat flow meter to perform steady-state measurements.

Thermal conductivity has been measured with a commercial heat flow meter (HFM method) (heat flux transducer area of $100 \times 100 \text{ mm}^2$) for four different insulating materials covering a range of thermal conductivities between 26 and $39 \text{ mW m}^{-1} \text{K}^{-1}$. The same samples (with dimensions $300 \times 300 \text{ mm}^2$) were measured with the self-developed external sensor method (ES method). In the ES method, two rubber pieces were placed between the sample and the plates to minimize the fluctuations of the heat flux registered by the sensor, and two thermocouples were used to monitor the temperature on both sides of the samples.

Results showed that the ES method provides slightly higher thermal conductivities than the HFM method.

Furthermore, the relative difference increase as the measurement temperature increases. The differences have been normalized by obtaining a calibration factor to improve the accuracy of the ES method. The effect of the sample size has been studied using XPS foam samples, obtaining good results with the ES method for sample sizes as small as $50 \times 50 \text{ mm}^2$. Finally, the method has been validated by measuring $50 \times 50 \text{ mm}^2$ samples of the rest of the materials (EPS, PUR, and PE foams). In general, once the correction is applied, the relative difference is reduced. Therefore, the developed external sensor method allows measuring the thermal conductivity (within the temperature range of the sensor) using a steady-state approach of small prototypes as those produced at lab-scale.

Supplementary Information The online version contains supplementary material available at <https://doi.org/10.1007/s10973-022-11457-7>.

Acknowledgements Financial support from the Junta of Castile and Leon Grant (I. Sánchez-Calderón) and FPU Grant FPU17/03299 (Beatriz Merillas) from the Spanish Ministry of Science, Innovation, and Universities are gratefully acknowledged. Financial assistance from the Spanish Ministry of Science, Innovation, and Universities (RTI2018-098749-B-I00 and PTQ2019-010560 (Victoria Bernardo-García)) is gratefully acknowledged. Financial support from the European Regional Development Fund of the European Union and the of Castile and Leon ((ICE): R&D PROJECTS IN SMEs: PAVIPEX. 04/18/VA/008 and M-ERA.NET PROJECT: FICACEL. 11/20/VA/0001) is gratefully acknowledged.

Author contributions Design of the experiment, I. Sánchez-Calderón and B. Merillas; thermal conductivity measurements, I. Sánchez-Calderón and B. Merillas; data analysis, I. Sánchez-Calderón; revision of the obtained results, I. Sánchez-Calderón, B. Merillas, V. Bernardo and M.Á. Rodríguez-Pérez; writing—original draft preparation, I. Sánchez-Calderón; writing—review and editing, B. Merillas, V. Bernardo and M.Á. Rodríguez-Pérez. All authors have read and agreed to the published version of the manuscript.

Funding Open Access funding provided thanks to the CRUE-CSIC agreement with Springer Nature.

Open Access This article is licensed under a Creative Commons Attribution 4.0 International License, which permits use, sharing, adaptation, distribution and reproduction in any medium or format, as long as you give appropriate credit to the original author(s) and the source, provide a link to the Creative Commons licence, and indicate if changes were made. The images or other third party material in this article are included in the article's Creative Commons licence, unless indicated otherwise in a credit line to the material. If material is not included in the article's Creative Commons licence and your intended use is not permitted by statutory regulation or exceeds the permitted use, you will need to obtain permission directly from the copyright holder. To view a copy of this licence, visit <http://creativecommons.org/licenses/by/4.0/>.

References

- Boermans T, Grözinger J, von Manteuffel B, Surmeli-Anac N, Jhon A, Leutgöb K, Bachner D. Assessment of cost optimal calculations in the context of the EPBD (ENER/C3/2013-414); 2015:177.
- Wu M, Huang HX. Enhancing thermal conductivity of PMMA/PS blend via forming affluent and continuous conductive pathways of graphene layers. *Compos Sci Technol*. 2021;206: 108668. <https://doi.org/10.1016/j.compscitech.2021.108668>.
- Costeux S. CO₂-Blown nanocellular foams. *J Appl Polym Sci*. 2014. <https://doi.org/10.1002/app.41293>.
- König J, Lopez-Gil A, Cimavilla-Roman P, Rodriguez-Perez MA, Petersen RR, Østergaard MB, Iversen N, Yue Y, Spreitzer M. Synthesis and properties of open- and closed-porous foamed glass with a low density. *Constr Build Mater*. 2020. <https://doi.org/10.1016/j.conbuildmat.2020.118574>.
- Diascorn N, Calas S, Sallée H, Achard P, Rigacci A. Polyurethane aerogels synthesis for thermal insulation—textural, thermal and mechanical properties. *J Supercrit Fluids*. 2015;106:76–84. <https://doi.org/10.1016/j.supflu.2015.05.012>.
- Yüksel N. The review of some commonly used methods and techniques to measure the thermal conductivity of insulation materials. *Insul Mater Context Sustain*. 2016. <https://doi.org/10.5772/64157>.
- Zhao D, Qian X, Gu X, Jajja SA, Yang R. Measurement techniques for thermal conductivity and interfacial thermal conductance of bulk and thin film materials. *J Electron Packag Trans ASME*. 2016;138:1–19. <https://doi.org/10.1115/1.4034605>.
- Kraemer D, Chen G. A simple differential steady-state method to measure the thermal conductivity of solid bulk materials with high accuracy. *Rev Sci Instrum*. 2014. <https://doi.org/10.1063/1.4865111>.
- Almanza O, Rodríguez-Pérez MA, De Saja JA. Applicability of the transient plane source method to measure the thermal conductivity of low-density polyethylene foams. *J Polym Sci Part B Polym Phys*. 2004;42:1226–34. <https://doi.org/10.1002/polb.20005>.
- Zheng Q, Kaur S, Dames C, Prasher RS. Analysis and improvement of the hot disk transient plane source method for low thermal conductivity materials. *Int J Heat Mass Transf*. 2020;151: 119331. <https://doi.org/10.1016/j.ijheatmasstransfer.2020.119331>.
- Jannot Y, Degiovanni A, Grigoroza-Moutiers V, Godefroy J. A passive guard for low thermal conductivity measurement of small samples by the hot plate method. *Meas Sci Technol*. 2017. <https://doi.org/10.1088/1361-6501/28/1/015008>.
- ASTM C518 Standard Test Method for Steady-State Thermal Transmission Properties by Means of the Heat Flow Meter Apparatus (2017).
- ISO 8301 Thermal insulation—Determination of steady-state thermal resistance and related properties—Heat flow meter (1991).
- ASTM C177: Standard Test Method for Steady-State Heat Flux Measurements and Thermal Transmission Properties by Means of the Guarded-Hot-Plate Apparatus (1997).
- ISO 8302 Thermal insulation—Determination of steady-state thermal resistance and related properties—Guarded hot plate apparatus, (1991). <https://standards.iteh.ai/catalog/standards/sist/11594d7b-fd5c-45d7-816b-8e35f1df4d95/iso-4832-1991>.
- UNE-EN 12667:2001 Thermal performance of building materials and products. Determination of thermal resistance by means of guarded hot plate and heat flow meter methods. Products of high and medium thermal resistance (2002).
- Jannot Y, Felix V, Degiovanni A. A centered hot plate method for measurement of thermal properties of thin insulating materials. *Meas Sci Technol*. 2010. <https://doi.org/10.1088/0957-0233/21/3/035106>.
- Jannot Y, Schaefer S, Degiovanni A, Bianchin J, Fierro V, Celzard A. A new method for measuring the thermal conductivity of small

- insulating samples. *Rev Sci Instrum.* 2019. <https://doi.org/10.1063/1.5065562>.
19. Miller RA, Kuczmariski MA. Method for measuring thermal conductivity of small highly insulating specimens. *J Test Eval.* 2010. <https://doi.org/10.1520/JTE102474>.
20. Pinto J, Solórzano E, Rodríguez-Perez MA, de Saja JA. Characterization of the cellular structure based on user-interactive image analysis procedures. *J Cell Plast.* 2013;49:555–75. <https://doi.org/10.1177/0021955X13503847>.
21. Schwyter ES, Helbling T, Glatz W, Hierold C. Fully automated measurement setup for non-destructive characterization of thermoelectric materials near room temperature. *Rev Sci Instrum.* 2012. <https://doi.org/10.1063/1.4737880>.

Publisher's Note Springer Nature remains neutral with regard to jurisdictional claims in published maps and institutional affiliations.

Authors and Affiliations

Ismael Sánchez-Calderón¹  · Beatriz Merillas¹ · Victoria Bernardo² · Miguel Ángel Rodríguez-Pérez^{1,3}

¹ Cellular Materials Laboratory (CellMat), Condensed Matter Physics Department, University of Valladolid, Campus Miguel Delibes, Paseo de Belén 7, 47011 Valladolid, Spain

² CellMat Technologies S.L., Paseo de Belén 9-A, 47011 Valladolid, Spain

³ BioEcoUVA Research Institute on Bioeconomy, University of Valladolid, 47011 Valladolid, Spain